ADAPTIVE FUZZY-SLIDING MODE CONTROLLER FOR A HELICOPTER-LIKE TWIN ROTOR MIMO SYSTEM

A. CHELIHI(1), M. TOUBA(2)

Automatic Department, Faculty of Engineering and Science, University of Mohamed Kheider, Biskra, Algeria
[a]chelihi.abdelghani@yahoo.fr, [b]tmostefa2005@yahoo.fr

ABSTRACT

This paper addresses the attitude control problem for a twin rotor unmanned helicopter driven by DC motors. The control objective is to have the helicopter attitude, i.e., pitch and yaw angles, track specified angles. From the considered dynamics of the plant, it is observed that the main difficulty of the control problem is due to the existing nonlinear coupling effects between the two perpendicular rotors. Hence, an adaptive control approach based on the fuzzy-sliding mode controller is developed to solve the problem. In the controller design, firstly, the twin rotor multiple-input multiple-output system (TRMS) is decoupled into two single-input–single-output systems, and the cross couplings can be considered as disturbances to each other. Then, a fuzzy-sliding mode controller is designed for each of them. The stability of the overall closed-loop system is proven to be asymptotically stable based on the Lyapunov theorem. In order to demonstrate the applicability of the proposed control scheme, computer simulations is shown.

.

KEYWORDS: Sliding control, adaptive control, fuzzy system, Lyapunov stability, TRMS system.

1. INTRODUCTION

Helicopters have been widely used in air traffic systems, especially in urgent transportation needs such as medical treatment rescues and life-saving goods transportations. In addition, missions like ground detection, traffic condition assessment, smuggling prevention, and crime precautions heavily depend on using helicopters. The TRMS setup is designed by Feedback Instruments Ltd which has some resemblances with a helicopter [1]. For instance, like a helicopter it has a strong cross- coupling between the main and tail rotors. It is a highly nonlinear and complex system. Some of its states and outputs are inaccessible for measurements. Thus, from the control perspective, it can be perceived as a challenging problem. The control objective is to move the beam of the TRMS as quickly and accurately as possible to the desired attitudes in terms of both the pitch and yaw angles.

In the literature, several research studies have been carried out for to design control systems for the TRMS test bed which most suggest a decoupling control scheme [2-14]. Some strategies ranging from classical to advanced and intelligent techniques have been developed [2–10]. For example, in [2] the pitch channel of the TRMS is considered for witch one degree of freedom inversion control is developed combined with an adaptive neural network to compensate for inversion errors. Decoupling control of TRMS using deadbeat robust control technique is reported in reference [3]. In that investigation, the extracted model is decoupled into two single-input single-output (SISO) systems for which a proportional–integral–derivative (PID)-based robust dead-beat controller has been applied. In [4, 5] authors presented the evolutionary computation based on genetic algorithm for the parameters optimization of the PID controller to the TRMS system. Model reference adaptive control for TRMS has been presented in reference [6], where a minimal controller synthesis (MCS) was utilized to TRMS system in decoupled control design. A comparison between classical control techniques and intelligent control based on fuzzy logic, and genetic algorithm is presented in [7]. In [8] parallel distributed fuzzy linear quadratic regulator controllers are designed to control the position of the pitch and yaw angles to cover various operating regions. All presented works consider the states of the TRMS available for measurement, however in [9] a predictive controller is developed where the states are estimated using unscented Kalman filter.

The sliding mode control (SMC), characterized by its robustness against non-linearity and parametric variations and its effectiveness in disturbance rejection [10], has been also used for the control of the TRMS system such as [11-14]. For instance, two-degree-of-freedom model for the TRMS is proposed using an optimal linear quadratic regulator (LQR) and a SMC in reference [11]. In [12-14] authors have applied a decentralized control method to a TRMS based on SMC. As the dynamics of TRMS pose

sufficient complexity as well as involve unknown nonlinearities, the main disadvantage of this control approach is its complexity, owing to the difficult differentiations of some complicated functions. In addition, implementing a sliding-mode controller in electrical systems is difficult because the chattering properties in high-frequency oscillations can damage the actuator.

Motivated by the ability of adaptive SMC to deal with uncertain nonlinear systems to achieve excellent closed-loop performance, an adaptive fuzzy-sliding mode control (AFSC) approach is developed for the TRMS. The advantage of controlling the system using the fuzzy logic technique is that the equivalent control laws derived of the model of the TRMS in [14], is approximated by a fuzzy system. In our design methodology, the TRMS is considered as a large-scale system which is decoupled into its vertical and horizontal two SISO subsystems. Then, an AFSMCs are designed for each subsystem which tuning laws are realised to deal with system uncertainty. Finally, the two controllers are applied to the original coupled TRMS. The stability of the overall closed-loop system is guaranteed based on the Lyapunov stability theory. The effectiveness of the proposed scheme is validated by simulations in which the proposed controller shows an excellent performance for both stabilization and tracking tasks.

2 MODEL DESCRIPTION OF THE TRMS

The TRMS, as shown in Fig. 1, is a laboratory test rig designed for control experiments by Feedback Instruments Limited [1]. Its behavior in certain aspects resembles that of a helicopter. This TRMS consists of a beam with main and tail rotors driven by direct current (DC) motors. The two rotors are controlled by variable speed electric motors enabling the TRMS to rotate in vertical plane (pitch denoted as θ_v) and horizontal plane (yaw denoted θ_h). The TRMS is constructed such that the angle of attack of the blades is fixed. Then, the aerodynamic force is controlled by varying the speed of the motors. The TRMS is characterized by cross-coupling (Fig. 2) complex dynamics, and it is noted that some of its states are not accessible for measurement.

The dynamic model as supplied by the manufacturer [1] is given for vertical movement by the following equations:

$$\dot{\theta}_v = \Omega_v = \mathrm{S}_v + \frac{J_{tr}\omega_t}{J_v} \tag{1}$$

$$\dot{S}_v = \frac{l_m F_v(\omega_m) + g\big((a-b)\cos\theta_v - e\sin\theta_v\big) - \Omega_v k_v + g_{hv}}{J_v} \tag{2}$$

Similarly, the horizontal movement is described by the following equations:

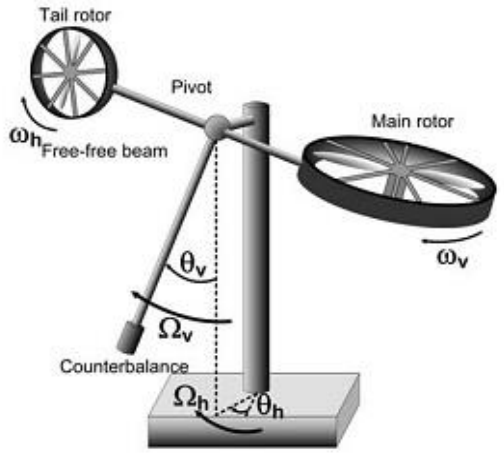

Figure 01: Twin Rotor MIMO System

$$\dot{\theta}_h = \Omega_h = \mathrm{S}_h + \frac{J_{mr}\omega_m \cos\theta_v}{J_h} \tag{3}$$

$$\dot{S}_h = \frac{l_t F_h(\omega_t)\cos\theta_v - \Omega_h k_h}{J_h} \tag{4}$$

where $\theta_v(\theta_h)$ is the pitch (yaw) angle of beam, $\Omega_v(\Omega_h)$ is the angular velocity around the vertical (horizontal) axis, $\omega_m(\omega_t)$ is the rotational velocity of the main (tail) rotor, $S_v(S_h)$ is the angular momentum in vertical (horizontal) plane of the beam, $J_{mr}(J_{tr})$ is the moments of inertia in DC-motor main (tail) propeller subsystem, $J_v(J_h)$ is the moment of inertia relative to vertical (horizontal) axis, and $k_v(k_h)$ is the friction constant of the main (tail) propeller rotors and g is gravitational acceleration, $F_v(F_h)$ is the dependence of the propulsive forces on DC-motors rotational speeds. The definitions and numerical values of the different constants and parameters are given in appendix. The propulsive forces F_v and F_h moving the joined beam in the horizontal and vertical direction, respectively, are described by a nonlinear functions of the angular velocity's ω_m and ω_t

$$F_v(\omega_m) = -3{,}48\cdot 10^{-12}\omega_m^5 + 1{,}09\cdot 10^{-9}\omega_m^4 + 4{,}123\cdot 10^{-6}\omega_m^3 - 1{,}632\cdot 10^{-4}\omega_m^2 + 9{,}544\cdot 10^{-2}\omega_m \tag{5}$$

$$F_h(\omega_t) = -3\cdot 10^{-14}\omega_t^5 - 1{,}595\cdot 10^{-11}\omega_t^4 + 2{,}511\cdot 10^{-7}\omega_t^3 - 1{,}808\cdot 10^{-4}\omega_t^2 + 0{,}0801\cdot\omega_t \tag{6}$$

where the rotational velocity ω_m and ω_t of main and tail propellers are a non-linear functions of a rotation angle of the main and tail DC motor

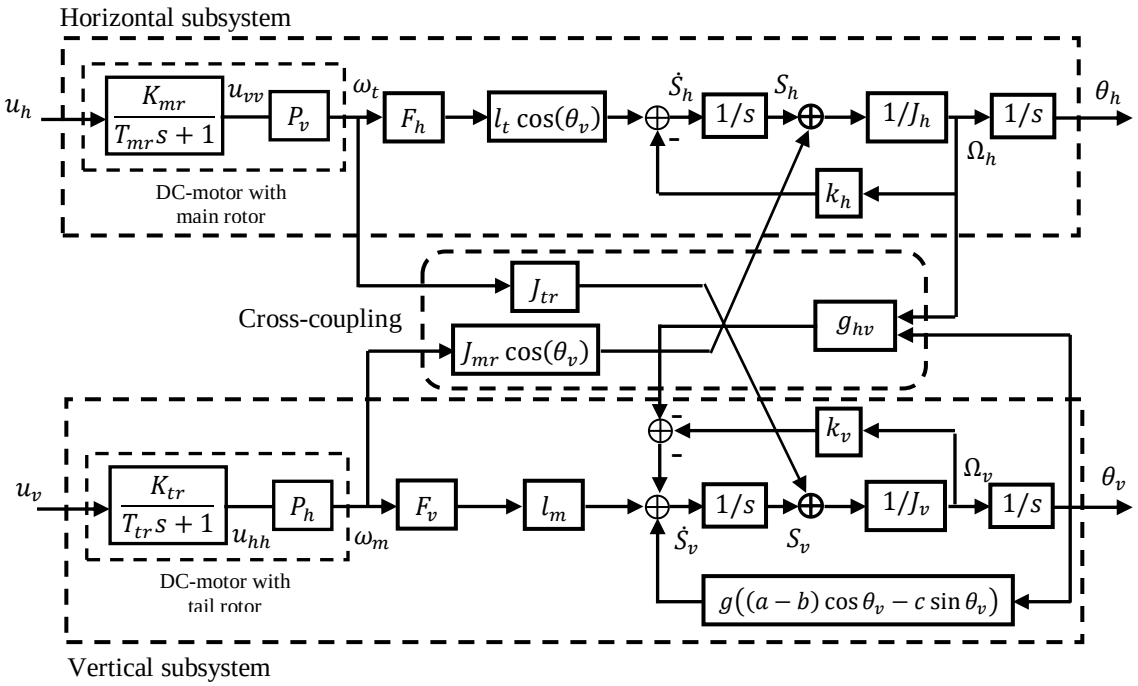

Figure 02: The MIMO block diagram of the TRMS

$$\omega_m = P_v(u_{vv}) = 90{,}99u_{vv}^6 + 599{,}73u_{vv}^5 - 129{,}26u_{vv}^4 - 1238{,}64u_{vv}^3 + 63{,}45u_{vv}^2 + 1283{,}41u_{vv} \quad (7)$$

$$\omega_t = P_h(u_{hh}) = 2020u_{hh}^5 - 194{,}69u_{hh}^4 - 4283{,}15u_{hh}^3 + 262{,}27u_{hh}^2 + 3796{,}83u_{hh} \quad (8)$$

with the main and tail motors and their electric control circuit approximated by a first-order transfer function, and thus, in Laplace domain, the motor momentums are described by

$$\frac{du_{vv}}{dt} = \frac{1}{T_{mr}}(-u_{vv} + K_{mr}u_v) \quad (9)$$

$$\frac{du_{hh}}{dt} = \frac{1}{T_{tr}}(-u_{hh} + K_{tr}u_h) \quad (10)$$

where $u_v(u_h)$ is the input voltage of the main (tail) DC motor, $T_{mr}(T_{tr})$ is the time constant of the main (tail) rotor and $K_{mr}(K_{tr})$ is the static gain of main (tail) DC motor.

A block diagram representation of the TRMS model is shown in Fig. 2). It is suitable for using in the SIMULINK environment [1]. The block diagram in Fig. 3 shows that the TRMS is a large-scale system composed of two interconnected nonlinear subsystems representing the dynamics of TRMS in horizontal and vertical planes.

The objective is to deal with the attitude stabilization of the TRMS beam in an arbitrary, within practical limits, desired position (yaw and pitch), or making it track a desired trajectory. Both goals may be achieved by means of the chosen controller of the next section.

3 ADAPTIVE FUZZY-SLIDING MODE CONTROLLER DESIGN

In this section, designing the adaptive fuzzy-sliding mode controller is considered. First, the TRMS model is decoupled into its two sub-models and considering the interconnections as model uncertainties and perturbations. Then a sliding mode control strategy is applied for each subsystem to achieve the control objective and to cancel the effect of the couplings. Finally, the adaptive fuzzy system is introduced to render the control laws of the TRMS system adaptive and independent of the model which the global stability is proved based on the Lyapunov theory.

3.1 TRMS model decoupling

Let us decouple the TRMS model where the sub-model in vertical plane is derived from the coupled model by setting the pitch angle $\theta_h = 0\,(rad)$ and putting $u_h = 0\,(V)$ in equations (1) and (2) which leads to $\omega_t = 0$. Thus, the model of the vertical subsystem of the TRMS is described by the following equations

$$\frac{d\theta_v}{dt} = \Omega_v \quad (11)$$

$$\frac{d\Omega_v}{dt} = \frac{l_m F_v(\omega_m) - \Omega_v k_v + g((A-B)\cos\theta_v + C\sin\theta_v)}{J_v} \quad (12)$$

where F_v and ω_m are given by (5) and (7) respectively.

In the same way as the vertical sub-model, the horizontal sub-model is obtained by setting the yaw angle $\theta_v = \theta_{v0}\ (rad)$ and putting $u_v = 0\ (V)$ in equation (3) and (4) which leads to $\omega_m = 0$. Hence, the following equations describe the horizontal model :

$$\frac{d\theta_h}{dt} = \Omega_h \quad (13)$$

$$\frac{d\Omega_h}{dt} = \frac{l_t F_h(\omega_t)\cos(\theta_{v0}) - K_h\Omega_h}{J_{h0}} \quad (14)$$

where $J_{h0} = D\sin^2\theta_{v0} + E\cos^2\theta_{v0} + F$, F_h and ω_t are given by (6) and (8) respectively.

To handle the parametric uncertainties and interaction between subsystems, the horizontal sub-model is extended with lumped disturbance torque ψ_v acting on the pitch axe, and satisfies the following inequalities

$$|\psi_v| \le \delta_v \text{ and } |\dot{\psi}_v| \le \eta_v \quad (15)$$

Where δ_v and η_v are known positive constants. As a result, using equations (9), (11) and (12), the extended nonlinear state space representation of the vertical sub-model is given by

$$\dot{x}_v = \begin{bmatrix} \dot{\theta}_v \\ \dot{\Omega}_v \\ \dot{u}_{vv} \end{bmatrix} = \begin{bmatrix} \Omega_v \\ \alpha_v(u_{vv}) - a_v\Omega_v + \beta_v(\theta_v) + d_v\psi_v \\ -c_v u_{vv} \end{bmatrix} + \begin{bmatrix} 0 \\ 0 \\ b_v \end{bmatrix} u_v \quad (16)$$

where $x_v = [\theta_v, \Omega_v, u_{vv}]^T$ a state vector of vertical subsystem and u_v is their input control, with

$a_v = \frac{K_v}{J_v}$, $b_v = \frac{K_{mr}}{T_{mr}}$, $c_v = \frac{1}{T_{mr}}$, $d_v = \frac{1}{J_v}$, $\alpha_v(u_{vv}) = \frac{l_m}{J_v}F_v\big(P_v(u_{vv})\big)$ and $\beta_v(\theta_v) = \frac{g}{J_v}((A-B)\cos\theta_v + C\sin\theta_v)$,

Similarly to the horizontal sub-model, using (10), (13) and (14) the nonlinear state space representation of the vertical sub-model is extended with bounded lumped disturbance torque ψ_h acting on the pitch axe, and satisfy the following inequalities

$$|\psi_h| \le \delta_h \text{ and } |\dot{\psi}_h| \le \eta_h \quad (17)$$

Where δ_h and η_h are known positive constants

Hence, the extended nonlinear state space vertical sub-model can be written as

$$\dot{x}_h = \begin{bmatrix} \dot{\theta}_h \\ \dot{\Omega}_h \\ \dot{u}_{hh} \end{bmatrix} = \begin{bmatrix} \Omega_h \\ \alpha_h(u_{hh}) - a_h\Omega_h + d_h\psi_h \\ -c_h u_{hh} \end{bmatrix} + \begin{bmatrix} 0 \\ 0 \\ b_h \end{bmatrix} u_h \quad (18)$$

where $x_h = [\theta_h, \Omega_h, u_{hh}]^T$ is a state vector of horizontal subsystem and u_h is their input control, with

$a_h = \frac{K_v}{J_{h0}}$, $b_h = \frac{K_{tr}}{T_{tr}}$, $c_h = \frac{1}{T_{tr}}$ $d_h = \frac{1}{J_{h0}}$ and $\alpha_h(u_{hh}) = \frac{l_t}{J_{h0}}F_h\big(P_h(u_{hh})\big)$.

These disturbance torques, i.e. ψ_v and ψ_h, account for bounded interactions between the two subsystems, parametric uncertainty, unmodelled dynamics and all disturbances affecting the system. Among these are non-modelled effects due to the supply cables and gyroscopic torques as well as the couplings caused by the tail rotor and the main rotor in the case of angular accelerations of the propellers.

3.2 Sliding mode controllers of the TRMS

The sliding mode controller is already developed by [14] to control a TRMS system in decentralized scheme which consisting of two interconnected SISO subsystem, horizontal and vertical. However, in this present work, the proof of singularity of the control laws is studied which makes its implementation possible. In addition, the proposed control laws have adaptive control gains in order to eliminate the chattering problem.

Let e_v and e_h denote the errors between the measured and the desired trajectories (denoted with a subscript *) for the yaw angle and the pitch angle according to

$$e_v = \theta_v - \theta_v^* \text{ and } e_h = \theta_h - \theta_h^* \quad (19)$$

Accurate tracking of desired trajectories for the pitch angle and the yaw angle and be achieved by the following choice of the sliding surfaces

$$S_i(x_i) = \left(\frac{d}{dt} + \lambda_i\right)^{n_i - 1} e_i,\ i \in [v, h] \quad (20)$$

where n_i is the relative degree of each subsystem, i.e. the degree of the vertical and horizontal sub-model, λ_i is the positive constant characterizing the dynamics of the sliding surfaces. Here, The sliding mode control can be divided into two phases: the sliding phase with $S_i(x_i) = 0$, $\dot{S}_i(x_i) = 0$

and the reaching phase with $S_i(x_i) \neq 0$. The control input during the ideal sliding mode represents the equivalent control $u_{eq,i}$, whereas an additional switching control action $u_{sw,i}$ provides a finite-time convergence to the sliding surfaces during the reaching phase. Subsequently, the overall control input u_i can be expressed as the sum of both terms

$$u_i = u_{eq,i} + u_{sw,i},\ i \in [v,h] \tag{21}$$

The differentiation of the sliding surfaces S_v and S_h with respect to time, and for $n_v = n_v = 3$, results in

$$\dot{S}_v(x_v) = \dddot{\theta}_v - \dddot{\theta}_v^* + 2\lambda_v\left(\ddot{\theta}_v - \ddot{\theta}_v^*\right) + \lambda_v^2\left(\dot{\theta}_v - \dot{\theta}_v^*\right) \tag{22}$$

$$\dot{S}_h(x_h) = \dddot{\theta}_h - \dddot{\theta}_h^* + 2\lambda_h\left(\ddot{\theta}_h - \ddot{\theta}_h^*\right) + \lambda_h^2\left(\dot{\theta}_h - \dot{\theta}_h^*\right) \tag{23}$$

The sliding condition implies that in steady state, for both subsystems, the output trajectory at all-time remain on the sliding surfaces, $S_v(x_v) = 0$ and $S_h(x_h) = 0$. By choosing strictly positive coefficients of the Hurwitz polynomial, it can be ensured that the closed-loop subsystems are asymptotically stable during the ideal sliding mode. In this case, the error dynamics is governed by

$$\ddot{e}_i + 2\lambda_i e_i + \lambda_i^2 e_i = 0\ ,\ i \in [v,h] \tag{24}$$

where the strictly positive coefficients $\lambda_v > 0$ and $\lambda_h > 0$ has to be chosen so as to make the characteristic equation (24) Hurwitz for both vertical and horizontal subsystems.
Then the pitch and yaw angles of the TRMS track exponentially their desired tracking signals.

Firstly, for the vertical subsystem, substituting the value of $\dddot{\theta}_v$ from (16) into (22), the rate of change $\dot{S}_v$ can be expressed as

$$\begin{aligned}\dot{S}_v(x_v) = {} & 2\lambda_v\ddot{e}_v + \lambda_v^2\dot{e}_v - \dddot{\theta}_v^* - c_v D_{u_{vv}}^{(1)}\alpha_v u_{vv} \\ & + b_v D_{u_{vv}}^{(1)}\alpha_v u_v - a_v(\alpha_v + \beta_v) \\ & + \left(D_{\theta_v}^{(1)}\beta_v + a_v^2\right)\Omega_v \\ & + d_v\left(\dot{\psi}_v - a_v\psi_v\right)\end{aligned} \tag{25}$$

Where $D_x^{(l)}y = \partial^l y/\partial x^l$ denote lth partial order derivative of y with respect to x. Thus, $D_{u_{vv}}^{(1)}\alpha_v$ and $D_{\theta_v}^{(1)}\beta_v$ are calculated according to:

$D_{u_{vv}}^{(1)}\alpha_v = \partial\alpha_v/\partial u_{vv} = \frac{l_m}{J_v}\nabla_v$, and

$\nabla_v = (\partial F_v/\partial F\omega_m)(\partial p_v/\partial u_{vv})$

$D_{\theta_v}^{(1)}\beta_v = \partial\beta_v/\partial\theta_v = \frac{g}{J_v}((B-A)\sin\theta_v + C\cos\theta_v)$.

In the case where the dynamic sub-models of the TRMS are assumed to be totally independent, i.e. without any modelling uncertainties and any effect of interactions between subsystems. Hence, for vertical subsystems with $\psi_v = 0$, and by setting $\dot{S}_v(x_v) = 0$ in equation (25), the equivalent control input voltage for vertical subsystem is obtained:

$$\begin{aligned}u_{eq,v} = \frac{-1}{b_v D_{u_{vv}}^{(1)}\alpha_v}\Big[& \upsilon_v - c_v D_{u_{vv}}^{(1)}\alpha_v u_{vv} - a_v(\alpha_v + \beta_v) + \\ & + \left(D_{\theta_v}^{(1)}\beta_v + a_v^2\right)\Omega_v\Big]\end{aligned} \tag{26}$$

where υ_v is the equivalent control input corresponds to the ideal motions of the vertical subsystem on the sliding surfaces $S_v(x_v) = 0$, with

$$\upsilon_v = \dddot{\theta}_v^* - \lambda_v^2\dot{e}_v - 2\lambda_v\ddot{e}_v \tag{27}$$

The obtained equivalent control for vertical subsystem is non-singular iff the term ∇_valong the operating space is nonzero, that is, is either positive or negative: $\nabla_v \neq 0$. Since ∇_v is computed in terms of ω_m and u_{vv} by using equations (5) and (7), its dynamics evolution is shown in Fig. 3. It is clear that $\nabla_v > 0$ which is the requirement condition to ensure the non-singularity, and hence to apply sliding mode control to the vertical subsystem.

Similar to the vertical sub-model, substituting the value of $\dddot{\theta}_h$ from (18) into (23), the rate of change $\dot{S}_h$ can be written as

$$\begin{aligned}\dot{S}_h(x_h) = {} & 2\lambda_h\ddot{e}_h + \lambda_h^2\dot{e}_h - \dddot{\theta}_h^* - c_h D_{u_{hh}}^{(1)}\alpha_h u_{hh} \\ & + b_h D_{u_{hh}}^{(1)}\alpha_h u_h - a_h(\alpha_h - a_h\Omega_h) \\ & + d_h\left(\dot{\psi}_h - a_h\psi_h\right)\end{aligned} \tag{28}$$

where $D_{u_{hh}}^{(1)}\alpha_h$ is partial derivative of α_h with respect to u_{hh} calculated according to:

$D_{u_{hh}}^{(1)}\alpha_h = \partial\alpha_h/\partial u_{hh} = \frac{l_t}{J_{h0}}\nabla_h$ and

$\nabla_h = (\partial F_h/\partial F\omega_t)(\partial p_h/\partial u_{hh})$

For any modelling uncertainties and any effect of interactions between sub-systems so that $\psi_h = 0$ and by setting $\dot{S}_h(x_h) = 0$ in equation (35), the equivalent control input voltage for horizontal subsystem is obtained

$$u_{eq,h} = \frac{-1}{b_h D_{u_{hh}}^{(1)}\alpha_h}\left[\upsilon_h - c_h D_{u_{hh}}^{(1)}\alpha_h u_{hh} - a_h(\alpha_h - a_h\Omega_h)\right] \tag{29}$$

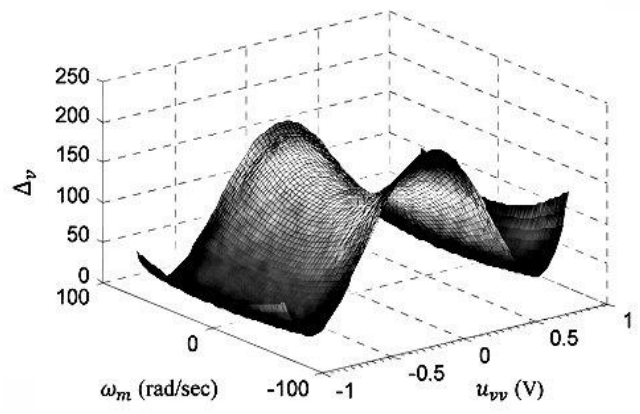

Figure 03: Dynamics evolution of ∇_v in terms of $\omega_m$and u_{vv}.

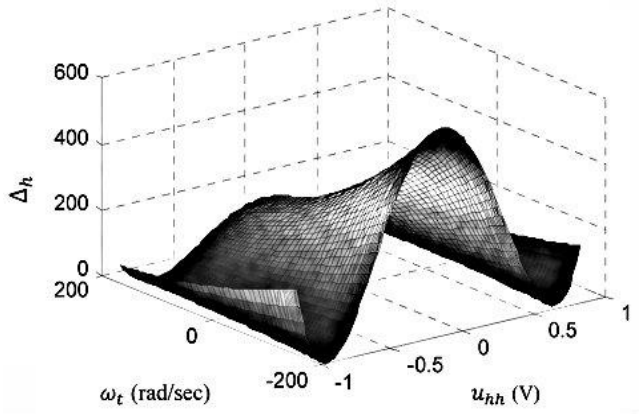

Figure 04: Dynamics evolution of ∇_h in terms of $\omega_t$and u_{hh}.

where v_h is the equivalent control input corresponds to the ideal motions of the horizontal subsystem on the sliding surface $S_h(x_h) = 0$, with

$$v_h = \ddot{\theta}_h^* - \lambda_h^2 \dot{e}_h - 2\lambda_h \ddot{e}_h \tag{30}$$

The obtained equivalent control for horizontal subsystem is non-singular iff the term ∇_halong the operating space is nonzero, that is, is either positive or negative: $\nabla_h \neq 0$. Since ∇_h is computed in terms of ω_t and u_{hh} by using equations (6) and (8), its dynamics evolution is shown in Fig. 4. It is clear that $\nabla_h > 0$ which is the requirement condition to ensure the non-singularity, and hence to apply sliding mode control to the vertical subsystem.

However, when the initial states are not located on the sliding surfaces and under the effect of disturbances, it is evident that the obtained equivalent controls laws (26) and (29) cannot be guarantee the stability of the closed-loop system and the boundedness of tracking errors.

So, an additional switching control part $u_{sw,i}$, $i = v, h$ to be designed in the next step brings the state back to the sliding surfaces – the reaching phase – and keeps it on the surfaces $S_i(x_i) = 0$ despite disturbances and uncertainties. So, the global control input voltages u_h and u_h are changed as follows:

$$u_v = \frac{-1}{b_v D_{u_{vv}}^{(1)} \alpha_v} \Big[v_v - c_v D_{u_{vv}}^{(1)} \alpha_v u_{vv} - a_v(\alpha_v + \beta_v) + \left(D_{\theta_v}^{(1)} \beta_v + a_v^2 \right) \Omega_v + K_v sgn(S_v) \Big] \tag{31}$$

$$u_h = \frac{-1}{b_h D_{u_{hh}}^{(1)} \alpha_h} \Big[v_h - c_h D_{u_{hh}}^{(1)} \alpha_h u_{hh} - a_h(\alpha_h - a_h \Omega_h) + K_h sgn(S_h) \Big] \tag{32}$$

where K_v and K_h are the adaptive control gains their updating laws will be given later in order to reduce the chattering phenomenon and guarantee the stability of the closed-loop system.

3.3 Stability analysis

To prove the asymptotic stability of the closed-loop system using the proposed decentralized sliding mode controller, let a Lyapunov function for the closed-loop system be chosen as

$$V = \frac{1}{2} S_v^2 + \frac{1}{2} S_h^2 + \frac{1}{2\gamma_v} K_v^2 + \frac{1}{2\gamma_h} K_h^2 \tag{33}$$

where γ_v and γ_h are any positive constants. By taking the time derivative of V, it is readily obtained that

$$\dot{V} = S_v \dot{S}_v + S_h \dot{S}_h + \frac{1}{\gamma_v} K_v \dot{K}_v + \frac{1}{\gamma_h} K_h \dot{K}_h \tag{34}$$

With substitution the expressions of (25), (28), (31) and (32), into (34), the following form is obtained

$$\dot{V} = S_v \left(d_v(\dot{\psi}_v - a_v \psi_v) - K_v sgn(S_v) \right) + S_h \left(d_h(\dot{\psi}_h - a_h \psi_h) - K_h sgn(S_h) \right) + \frac{1}{\gamma_v} K_v \dot{K}_v + \frac{1}{\gamma_h} K_h \dot{K}_h \tag{35}$$

Considering the assumptions made on the disturbances torques, then simply

$$\dot{V} \leq d_v(\eta_v - a_v \delta_v)|S_v| + d_h(\eta_h - a_h \delta_h)|S_h| + K_v \left(\frac{1}{\gamma_v} \dot{K}_v - |S_v| \right) + K_h \left(\frac{1}{\gamma_h} \dot{K}_h - |S_h| \right) \tag{36}$$

By choosing the following adaptations laws:

$$\dot{K}_v = \gamma_v |S_v| \tag{37}$$

$$\dot{K}_h = \gamma_h |S_h| \tag{38}$$

The derivative of V becomes:

$$\dot{V} \leq d_v(\eta_v - a_v\delta_v)|S_v| + \varepsilon_h d_h(\eta_h - a_h\delta_h)|S_h| \tag{39}$$

From equation (39) it can be concluded that the reaching condition and hence the stability of wool closed-loop system is obtained from $a_v > \eta_v\delta_v^{-1}$ and $a_h > \eta_h\delta_h^{-1}$. Therefore, by invoking Barbalat's lemma and Lyapunov theorem, all the signals inside the closed-loop system are bounded, and S_v, S_h, e_v, $e_h$will converge to zero asymptotically.

3.4 Fuzzy controllers

In this section, in order to eliminate the chattering problem and the dependence of control laws at parametric uncertainty of system, an adaptive fuzzy compensator is used to estimate de non-linearity functions in sliding mode controllers. Combining the Fuzzy Logic Control (FLC) with the adaptive SMC in equations. (31) and (32) results in developing the proposed AFSMC methodology [15]. The main advantage of this method is that the robust behavior of the system is guaranteed. The second advantage of the proposed AFSMC is that the performance of the system in the sense of removing chattering is improved in comparison with the same SMC technique without using FLC [16].

The output of the fuzzy system is calculated as [17]:

$$\hat{y}_{FC} = \hat{\theta}_{FC}^T \psi_{FC}(x) \tag{40}$$

where the $\hat{\theta}_{FC} = \left[\hat{\theta}_{FC}^1, \dots, \hat{\theta}_{FC}^N\right]^T$ is the vector parameters and $\psi_{FC}(x)$ is he regressor vector of the proposed fuzzy model given as follows:

$$\psi_{FC}(x) = [\varphi_F(x_1), \dots, \varphi_F(x_n)]^T \tag{41}$$

where $\varphi_F(\cdot)$ denotes the fuzzy basis functions calculated according to:

$$\varphi_F(x_i) = \frac{\prod_{i=1}^{n} \mu_{A_i^l}(x_i)}{\sum_{l=1}^{M}\left(\prod_{i=1}^{n} \mu_{A_i^l}(x_i)\right)} \tag{42}$$

where $\mu_{A_i^l}(x_i)$ are the membership functions of fuzzy sets A_i^l, $i = 1,..,n$, $l = 1, \dots M$ which are selected generally as Gaussian membership functions. It has been proven that fuzzy systems in the form of (40) can approximate continuous function on a compact domain to an arbitrary degree of accuracy if enough number of rules is given.

To counteract the effect of switching actions introduced by the sgn function, a smooth switching functions $tanh(S_i/\varepsilon_i)$ with a strictly positive constant ε_i, influencing a boundary layer thickness, are utilized. The chattering reduction depends on value of ε_i at the cost of robustness.

Hence, the input control voltages of the TRMS becomes

$$\hat{u}_v = \frac{-1}{\hat{f}_{1v}(x_v)}\left[\upsilon_v - \hat{f}_{2v}(x_v) + K_v tanh(S_v/\varepsilon_v)\right] \tag{43}$$

$$\hat{u}_h = \frac{-1}{\hat{f}_{1h}(x_h)}\left[\upsilon_h - \hat{f}_{2h}(x_h) + K_h tanh(S_h/\varepsilon_h)\right] \tag{44}$$

where $\hat{f}_{1v}(x_v)$, $\hat{f}_{2v}(x_v)$, $\hat{f}_{1h}(x_h)$ and $\hat{f}_{2h}(x_h)$ are the fuzzy approximators of nonlinear functions $b_v D_{u_{vv}}^{(1)}\alpha_v$, $c_v D_{u_{vv}}^{(1)}\alpha_v u_{vv} + a_v(\alpha_v + \beta_v) - \left(D_{\theta_v}^{(1)}\beta_v + a_v^2\right)\Omega_v$, $b_h D_{u_{hh}}^{(1)}\alpha_h$ and $c_h D_{u_{hh}}^{(1)}\alpha_h u_{hh} + a_h(\alpha_h - a_h\Omega_h)$ respectively, with

$$\begin{aligned}
\hat{f}_{1v}(x_v) &= \hat{\theta}_{1v}^T \psi_v(x_v) \\
\hat{f}_{2v}(x_v) &= \hat{\theta}_{2v}^T \psi_v(x_v) \\
\hat{f}_{1h}(x_h) &= \hat{\theta}_{1h}^T \psi_h(x_h) \\
\hat{f}_{2h}(x_h) &= \hat{\theta}_{2h}^T \psi_h(x_h)
\end{aligned} \tag{45}$$

The parameters $\hat{\theta}_{1v}$, $\hat{\theta}_{2v}$, $\hat{\theta}_{1v}$ and $\hat{\theta}_{2v}$ are optimized adaptively during the control process so that the stability of closed-loop system is proved using Lyapunov method [18]. This can be achieved if the following update law is adopted:

$$\begin{aligned}
\hat{\theta}_{1v} &= -\alpha_{1V}\int_0^t y_{ev}(t)\psi_v(x_v)dt - \beta_{1V}y_{ev}(t)\psi_v(x_v) \\
\hat{\theta}_{2v} &= -\alpha_{2v}\int_0^t y_{ev}(t)\psi_v(x_v)dt - \beta_{2V}y_{ev}(t)\psi_v(x_v) \\
\hat{\theta}_{1h} &= -\alpha_{1h}\int_0^t y_{eh}(t)\psi_h(x_h)dt - \beta_{1h}y_{eh}(t)\psi_h(x_h) \\
\hat{\theta}_{2h} &= -\alpha_{2h}\int_0^t y_{eh}(t)\psi_h(x_h)dt - \beta_{2h}y_{eh}(t)\psi_h(x_h)
\end{aligned} \tag{46}$$

where $y_{ei} = e^T P_{ni}$, and $P_{ni} = \Gamma P_i$ for $i = v, h$ is the last column of the Lyapunov matrix P_i. α_{iV}, α_{ih}, β_{1V} and β_{ih}, $j = 1,2$ are positive adaptation weights [19].

The block diagram of the TRMS control system with the proposed controllers is shown in Fig. 5.

4 SIMULATION RESULTS

To show the performance of the proposed control scheme, simulations tests on the phenomenological model of the TRMS system are carried out, with the parameters given in Table A1 (Appendix).

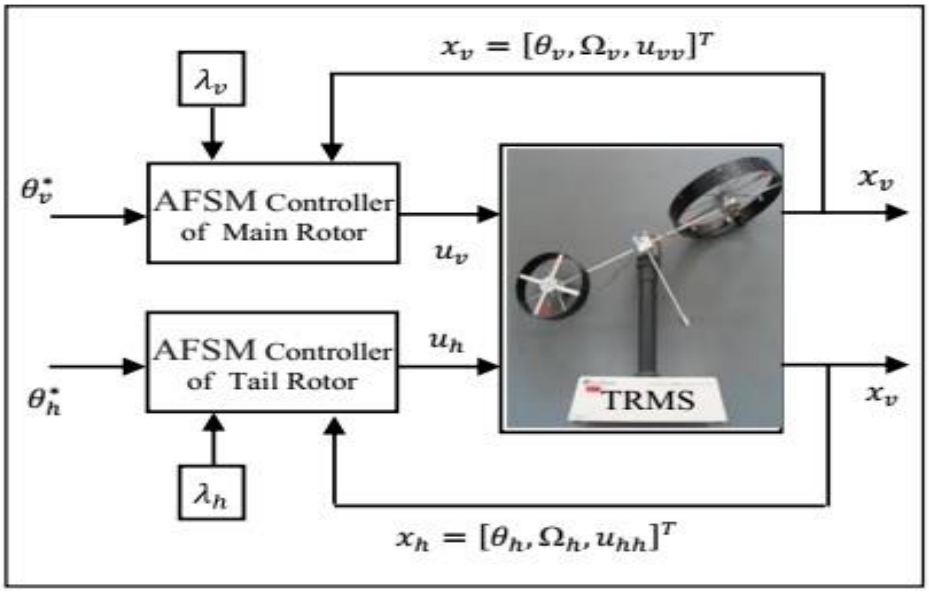

Figure 05 : Block diagram of the proposed adaptive fuzzy-sliding mode (AFSM) controller scheme for TRMS system.

Different reference signals are used for regulation and the tracking problems following different scenarios presented in [12]. Where all tests are performed using the same initial states $x_v = [-0.63, 0, 0]^T$ and $x_h = [0, 0, 0]^T$ which represent the static equilibrium point at rest with stopped main and tail DC-motors. In addition, robustness of these controllers against external disturbances and changes in the system parameters will be evaluated.

The design parameters are chosen for both horizontal and vertical controllers as $\alpha_{iV} = \beta_{iV} = 0.1$ for $i = 1,2$, $\gamma_v = \gamma_h = 2.5$ and $\varepsilon_v = \varepsilon_h = 0.5$. These values have been determined through numerical simulation tests, and were found to work well under all conditions. Considering the value of a_v and a_h with the range of interest of disturbance torques acting on the TRMS system, it is reasonable to assume that the stability conditions are fulfilled. The membership functions for system state x_i for $i = v, h$ are chosen as :

$\mu_{F_1^1}(x_i) = 1/(1 + exp(11(x_i + 1))$,

$\mu_{F_1^2}(x_i) = \exp\{-(x_i + 0.3)^2\}$,

$\mu_{F_1^3}(x_1) = \exp\{-(x_i)^2\}$,

$\mu_{F_1^4}(x_i) = \exp\{-(x_i - 0.3)^2\}$,

$\mu_{F_1^5}(x_1) = 1/(1 + exp(-11(x_i - 1))$.

In simulation tests using MATLAB and Simulink, the proposed controllers have proven to be reliable with respect to different reference signals that cover various operating regions. The TRMS responses are sketched in Figs. 6 to 9. Fig. 6 shows the responses of the control system according to square reference signals with different frequencies for pitch and yaw angles. Fig. 7 depicte the performance of the controller for sine reference signals with different frequencies. Fig. 8 gives the angles responses of the TRMS, with respect to different reference signals with different frequencies to show the effectiveness of the proposed control system to deal with different interactions of the two channels.

To evaluate the robustness of the controller, parametric variations and external disturbances were introduced. The parametric variation is introduced by changing the position of the counterweight shown in Fig. 1 in the pendulum counterweight. For the external disturbances, an external force is applied to the system at 40 and lasts for 100 sec. The results of a sinusoidal reference signal tracking is depicted in Fig. 9 which shows that the controller is immune against parameter variations and recovers adequately for the external perturbation. The peaking phenomenon appears in the input voltages u_v and u_h, as show in Fig. 9(c) and (d), represents the transient of the adaptation to compensate the sudden change of TRMS angles caused by perturbations.

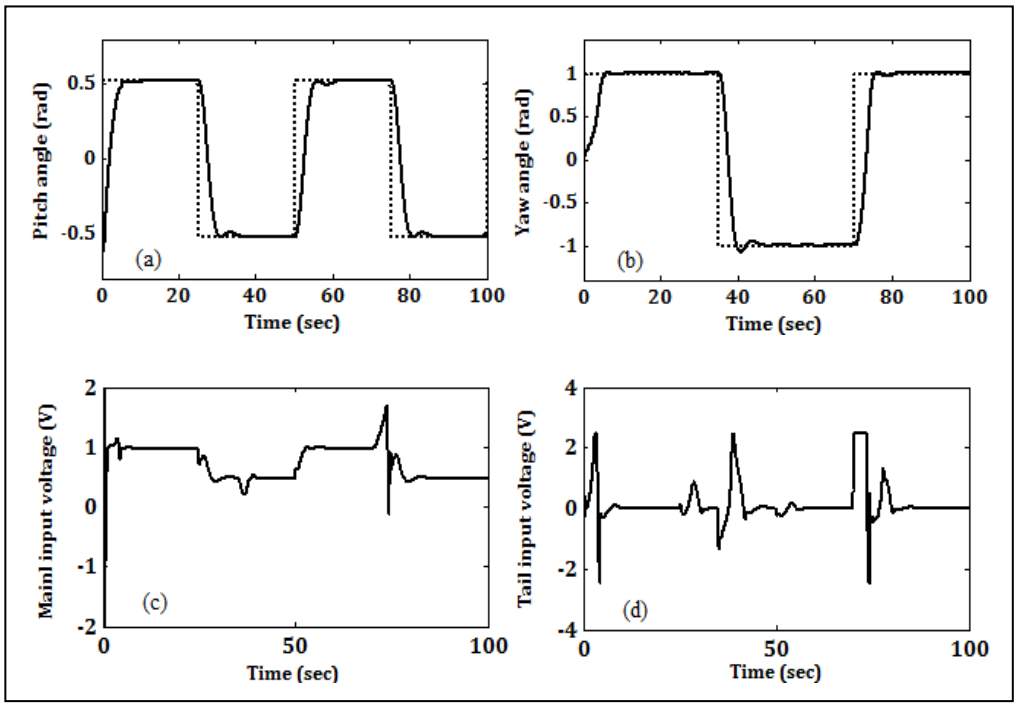

Figure 06: Simulation results for square wave references. (a) pitch angle θ_v (solid line) and reference θ_v^* (dotted line), (b) yaw angle θ_h (solid line) and reference θ_h^* (dotted line), (c) main input voltage, (d) tail input voltage.

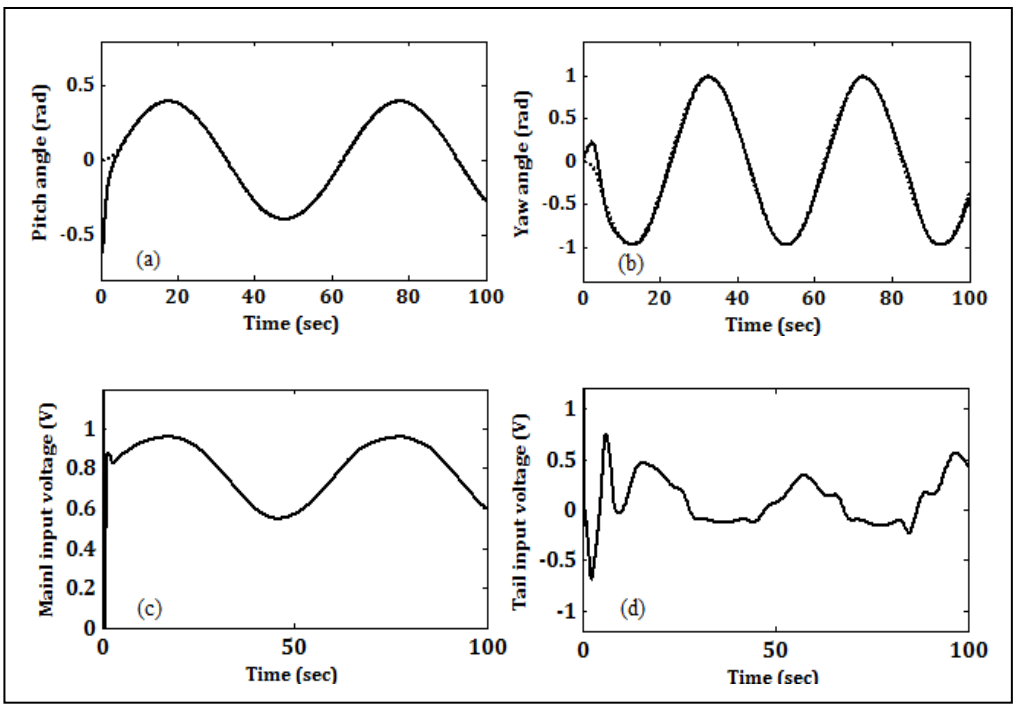

Figure 07: Simulation results for sine wave references. (a) pitch angle θ_v (solid line) and reference θ_v^* (dotted line), (b) yaw angle θ_h (solid line) and reference θ_h^* (dotted line), (c) main input voltage, (d) tail input voltage.

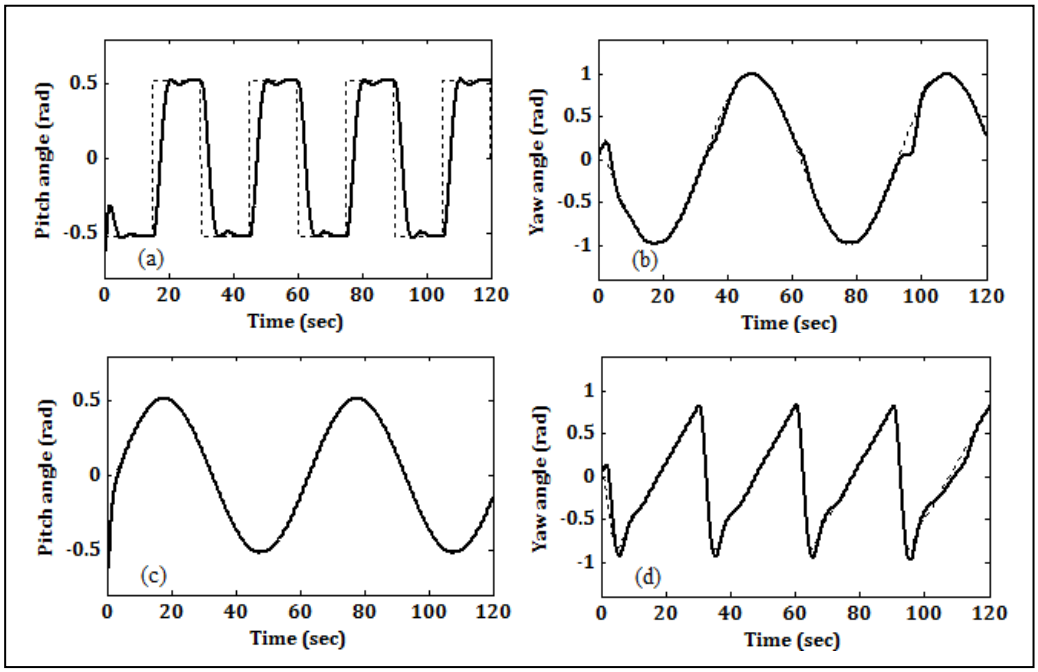

Figure 08: Angles responses for differences frequencies. (a) square wave reference for pitch angle, (b) and (c) sine wave reference for pitch and yaw angles, (d) sawtooth wave reference for yaw angle.

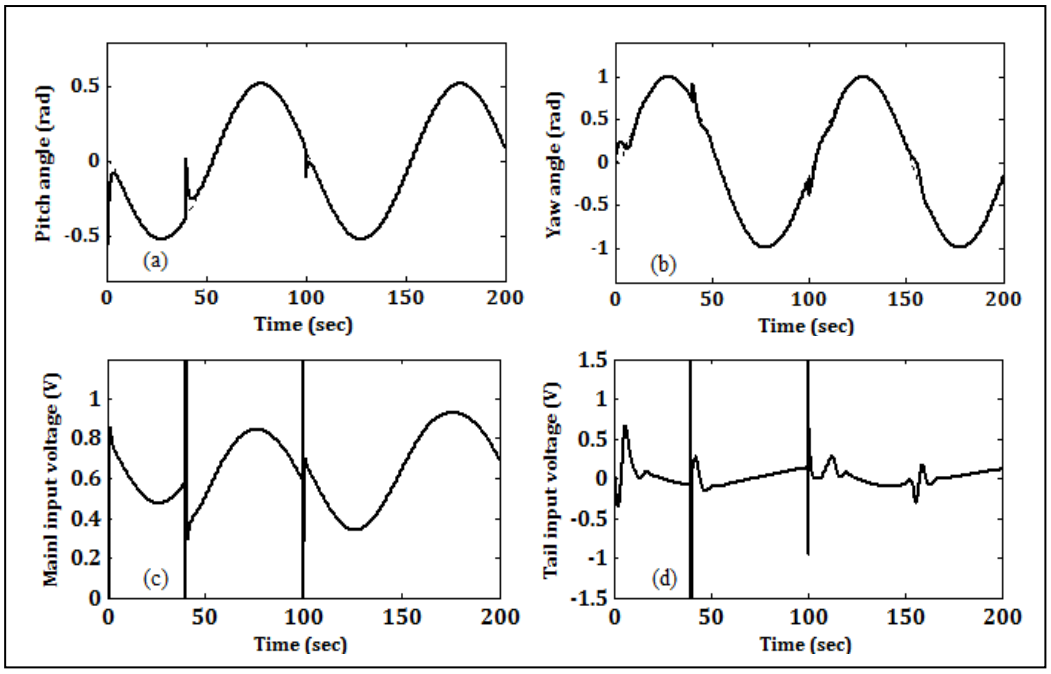

Figure 09: Simulation results for sine wave references in robust test. (a) pitch angle θ_v (solid line) and reference θ_v^* (dotted line), (b) yaw angle θ_h (solid line) and reference θ_h^* (dotted line), (c) main input voltage, (d) tail input voltage.

5 CONCLUSION

In this investigation, an adaptive fuzzy-sliding mode controller (AFSMC) has been developed to the TRMS system whose dynamics resemble that of a helicopter. The extracted model of TRMS has been decoupled into two SISO systems which the proposed AFSMC is applied for each of them. This approach does not require a good knowledge of the model and is simple to implement. It leads to a very quick and efficient optimization technique.
The components of the control laws for the two subsystems are derived through Lyapunov stability analysis. This design can tolerate the effect of system parameter variations and the cross-couplings between subsystems without degrading system performance. The proposed controller is applied to the system in simulation environment and the results show the efficacy of such a controller.

REFERENCES

[1] Twin Rotor MIMO System. Advanced teaching manual (33-007-04M5). Crowborough, E. Sussex, UK: Feedback Instruments Limited, 1998.

[2] A. Rahideh, M. H. Shaheed and A. H. Bajodah (2007) Adaptive nonlinear model inversion control of a twin rotor system using artificial intelligence. *Proc Inst. Mech. Eng G: J. Aerosp. Eng* 221(3):343–51.

[3] P. Wen and T. W. Lu (2008) Decoupling control of a twin rotor MIMO system using robust deadbeat control technique. *IET Control Theory Applications* 2(11): 999–1007.

[4] J. G. Juang, M. T. Huang and W. K. Liu (2008) PID control using presearched genetic algorithms for a MIMO system. *IEEE Trans. Syst. Man Cybern*: Part C 38, 716–727.

[5] J. G. Juang, W. K. Liu and R. W. Lin (2011) A hybrid intelligent controller for a twin rotor MIMO system and its hardware implementation. *ISA Trans* 50 : 609–619.

[6] A. Chelihi and M. Chemachema (2014) Model reference adaptive control for twin rotor multiple-input and multiple-output system via minimal controller synthesis. *Proc Inst Mech Eng I: J Syst Control Eng* 228(6):406–18.

[7] J. G. Juang, R. W. Lin and W. K. Liu (2008) Comparison of classical control and intelligent control for a MIMO system. *Appl. Math. Comput*. 205, 778–791.

[8] C. W. Tao, J. S. Taur and Y. C. Chen (2010) Design of a parallel distributed fuzzy LQR controller for the twin rotor multi-input multi-output system. *Fuzzy Sets Syst* 161:2081–103.

[9] A. Rahideh and M. H. Shaheed (2012) Constrained output feedback model predictive control for nonlinear systems. Control. *Eng. Pract*. 20(4), 431–443.

[10] C. Edwards and S. K. Spurgeon (1998). *Sliding Mode Control*. Taylor and Francis, London.

[11] G. R. Yu and H. T. Liu (2005) Sliding mode control of a two-degree-of freedom helicopter via linear quadratic regulator. *Proc. IEEE Int. Conf. Syst. Man Cybern.*, 2005, vol. 4, pp. 3299–3304.

[12] A. K. Ekbote, N. S. Srinivasan and A. D. Mahindrakar (2011) Terminal Sliding Mode Control of a Twin Rotor Multiple-Input Multiple-Output System. *In Proceedings of the 18th World Congress The Inter. Fed. of Aut. Control Milano (Italy) August 28 - September 2*, pp. 952-957.

[13] S. Mondal and C. Mahanta (2012) Adaptive second-order sliding mode controller for twin rotor multi-input multi-output system. IET Control Theory and Applications, 6(14) : 2157-2167.

[14] F. Faris, A. Moussaoui, D. Boukhetala and (2017) Design and real-time implementation of a decentralized sliding mode controller for twin rotor multiple-input and multiple-output system via minimal controller synthesis. *Proc Inst Mech Eng I: J Syst Control Eng* 231(1) : 3–13.

[15] H. Ho, Y. Wong, and A. Rad (2009). Adaptive Fuzzy Sliding Mode Control with Chattering Elimination for Nonlinear SISO Systems . *Simulation Modeling Practice and Theory*, 17, 1199-1210.

[16] Chaouch D. E., Z. A. Foitih and M. F. Khelfi (2011) A self-tuning fuzzy inference sliding mode control scheme for a class of nonlinear systems. *Journal of Vibration and Control*, 18(10) 1494–1505.

[17] K. M. Passino and S. Yurkovitch **(**1998) *Fuzzy Control*. California: Addison Wesley Longman.

[18] Spooner J.T. & Passino K. M. (1997). Indirect adaptive fuzzy control for a class of decentralized systems. *American Control Conference* (*ACC),(1)* 2863-2867, Albuquerque, NM.

[19] Landau Y. D. (1979). *Adaptive control, the model reference approach.* New York: Marcel Dekker.

APPENDIX

The moment of the centrifugal forces (g_{hv}) corresponding to the motion of the beam around the vertical axis and the non-linear function of moment of inertia (J_h) with respect to vertical axis is expressed by the following equations:

$$g_{hv} = 0.5\Omega_h^2(a+b+c)\sin 2\theta_v \quad \text{(A1)}$$

$$J_h = d\sin^2\theta_v + e\cos^2\theta_v + f \quad \text{(A2)}$$

$$a = \left(\frac{m_t}{2} + m_{tr} + m_{ts}\right) l_t$$

$$b = \left(\frac{m_m}{2} + m_{mr} + m_{ms}\right) l_m,$$

$$c = \frac{m_b}{2} l_b + m_{cb} l_{cb}$$

$$d = \left(\frac{m_m}{3} + m_{mr} + m_{ms}\right) l_m^2 + \left(\frac{m_t}{3} + m_{tr} + m_{ts}\right) l_t^2$$

$$e = \frac{m_b}{2} l_b^2 + m_{cb} l_{cb}^2$$

$$f = m_{ms} r_{ms}^2 + \frac{m_{ts}}{2} r_{ts}^2$$

where $m_{ts/ms}$ is the mass of the tail/main shield, $r_{ts/ms}$ is the radius of the tail/main shield, $m_{t/m}$ is the mass of the tail/main part of the beam and $m_{tr/mr}$ is the mass of the tail/main DC-motor. m_b and l_b are the mass and the length of the counterweight beam, respectively. m_{cb} and l_{cb}

represent the mass of the counterweight and the distance between the counterweight and the joint, respectively. The numerical values of the parameters of the TRMS are given in Table A1.

Table A1: The TRMS parameters

Parameter	Value	Parameter	Value
l_t (m)	0.250	m_{ts} (kg)	0.165
l_m (m)	0.240	m_{ms} (kg)	0.225
l_b (m)	0.260	g (m/s^2)	9.81
l_{cb} (m)	0.130	J_v (kg.m^2)	0.055448
r_{ts} (m)	0.100	J_{tr} (kg.m^2)	1.6543 10^{-5}
r_{ms} (m)	0.155	J_{mr} (kg.m^2)	2.65 10^{-5}
m_{tr} (kg)	0.206	T_{mr}	1.432
m_{mr} (kg)	0.228	T_{tr}	0.3842
m_{cb} (kg)	0.068	K_{mr}	1
m_t (kg)	0.0155	K_{tr}	1
m_m (kg)	0.0145	K_v	0.00545371
m_b (kg)	0.022	K_h	0.0095